Monthly Notices of the ROYAL ASTRONOMICAL SOCIETY

MNRAS **549,** 1–7 (2026)
Advance Access publication 2026 May 4

https://doi.org/10.1093/mnras/stag842

A bright wideband radio burst from the isolated neutron star 2XMM J104608.7−594306

J. Tian [1★] K. M. Rajwade [2★] I. Pastor-Marazuela [1,3,4] B. W. Stappers [1] M. Caleb,[5,6] K. Shaji,[5,6] S. Singh,[1] E. D. Barr[7] and M. Kramer [7]

[1]*Jodrell Bank Centre for Astrophysics, Department of Physics and Astronomy, The University of Manchester, Manchester M13 9PL, UK*
[2]*Astrophysics, The University of Oxford, Denys Wilkinson Building, Keble Road, Oxford OX1 3RH, UK*
[3]*ASTRON, the Netherlands Institute for Radio Astronomy, Oude Hoogeveensedijk, 4, NL-7991 PD Dwingeloo, the Netherlands*
[4]*Anton Pannekoek Institute, University of Amsterdam, Amsterdam, the Netherlands*
[5]*Sydney Institute for Astronomy, School of Physics, The University of Sydney, NSW 2006, Australia*
[6]*ARC Centre of Excellence for Gravitational Wave Discovery (OzGrav), Hawthorn, 3122 Victoria, Australia*
[7]*Max-Planck-Institut für Radioastronomie, D-53121 Bonn, Germany*

Accepted 2026 May 1. Received 2026 April 30; in original form 2026 March 27

ABSTRACT

We present the discovery of a second coherent radio burst from the thermally emitting neutron star 2XMM J104608.7−594306 in our follow-up observations with the Murriyang Ultra-Wideband Low receiver. This burst shows complex morphology with multiple components and wideband emission spanning from 704 to 4032 MHz. We measured a steep spectral index of $\alpha = -2.18 \pm 0.16$. Our polarimetric analysis demonstrates that the burst is highly polarized with a linear and circular polarization fraction of 54 per cent and 22 per cent, respectively. We identified an orthogonal jump in the polarization position angles of the burst, resembling those seen in radio pulsars. We compared this burst with the first radio burst detected from the source with MeerKAT. These two bursts detected in a total of 40 h on source with MeerKAT and Murriyang, combined, show that 2XMM J104608.7−594306 can emit sporadic radio emission with luminosity jumps comparable to those seen in the bright bursts from SGR 1935+2154. This suggests that previously thought radio-quiet neutron stars such as X-ray dim isolated neutron stars and central compact objects could exhibit rare radio bursting activity.

Key words: stars: neutron – pulsars: general – radio continuum: transients.

1 INTRODUCTION

The neutron star (NS) zoo consists of different types of NSs, including rotation-powered radio pulsars, highly magnetized NSs (magnetars), X-ray dim isolated NSs (XDINSs) and central compact objects (CCOs). As individual classes, they differ in observational characteristics such as their electromagnetic spectrum and time intermittency and variability. While radio emission is prevalent in the manifestation of NSs, as observed from radio pulsars and some magnetars, until recently XDINSs and CCOs were thought to be radio-quiet (V. I. Kondratiev et al. 2009; S. Zane et al. 2011; I. Pastor-Marazuela et al. 2023a; W.-J. Lu et al. 2024; J. Kurpas et al. 2025). The discovery of very faint radio emission from the CCO 1E 1207.4−5209 in the supernova remnant G296.5+10.0 challenged this paradigm (L. Zhang et al. 2025). In contrast, the recent serendipitous discovery of a coherent radio burst with MeerKAT from 2XMM J104608.7−594306, an XDINS candidate discovered by *XMM–Newton* through its thermal X-ray emission (A. M. Pires et al. 2009, 2012, 2015), shows that XDINSs are capable of producing sporadic radio bursts similar to those seen from magnetars (K. M. Rajwade et al. 2025).

XDINSs are characterized by quasi-blackbody soft X-ray emission without persistent radio counterparts and lack of association to a supernova remnant. The first seven XDINSs, known as 'The Magnificent Seven', were discovered in ROSAT All-Sky Survey (RASS) data and located at a distance of $\lesssim 500$ pc (F. Haberl 2007). They share similar properties, including thermal X-ray spectra with effective temperatures of ∼40–100 eV, low X-ray luminosities of $\sim 10^{31}$ erg s^{-1}, low absorption column densities of $\sim 10^{20}$ cm^{-2}, long rotation periods of ∼3–10 s, strong magnetic fields of $\sim 10^{13}$ G and very faint optical counterparts with *B*-band magnitudes $\gtrsim 25$ (corresponding to X-ray-to-optical flux ratios $\gtrsim 10^4$). 2XMM J104608.7−594306 is an X-ray source discovered by *XMM–Newton* in the Carina Nebula (A. M. Pires et al. 2009). The X-ray observations revealed a purely thermal spectrum with a blackbody temperature of ≈135 eV and an absorbing column of $\approx 3 \times 10^{21}$ cm^{-2}. Deep optical follow-up observations yielded a very high X-ray-to-optical flux ratio of $> 10^{3.8}$ (A. M. Pires et al. 2012). These properties are remarkably reminiscent of XDINSs though no X-ray pulsation was firmly detected (A. M. Pires et al. 2015). The first confirmed radio emission from 2XMM J104608.7−594306 (K. M. Rajwade et al. 2025) suggests

★ E-mail: jun.tian@manchester.ac.uk (JT); kaustubh.rajwade@physics.ox.ac.uk (KMJ)

that the dearth of radio detection of XDINSs could be caused by unfavourable beaming geometry or highly intermittent emission, rather than intrinsic suppression of the radio emission. This is also supported by the similar X-ray properties observed between a persistent radio pulsar PSR J0726−2612 and XDINSs (M. Rigoselli et al. 2019).

XDINSs could be evolutionarily associated with magnetars given their similarly high X-ray luminosities and long spin periods (V. M. Kaspi 2010; T. Yoneyama et al. 2019). The analysis of the bright radio burst detected from 2XMM J104608.7−594306 revealed more similarities between this source and the magnetar population (K. M. Rajwade et al. 2025). Its radio luminosity reached $\sim 4.6 \times 10^{29}$ erg s^{-1}, similar to the average radio luminosity of radio-emitting magnetars (P. Esposito, N. Rea & G. L. Israel 2021). The temporal structure observed in this burst consists of at least eight distinct sub-components, resembling the quasi-periodic microstructure seen in magnetars and other NS populations (M. Kramer et al. 2024). Finding more radio bursts from 2XMM J104608.7−594306 could potentially reveal more similarities between this object and magnetars. In addition, since magnetars are thought to be plausible progenitors of fast radio bursts (FRBs; C. D. Bochenek et al. 2020; CHIME/FRB Collaboration 2020), XDINSs might be able to produce FRB-like bursts. However, we need to find radio bursts much brighter than the one detected from 2XMM J104608.7−594306 to test this scenario.

In this work, we present further follow-up observations on studies of 2XMM J104608.7−594306 with the ultrawide bandwidth low-frequency (UWL; 704–4032 MHz) receiver on the 64-m Murriyang radio telescope (G. Hobbs et al. 2020). We detect a second radio burst from 2XMM J104608.7−594306, which is brighter than the first one and shows extremely broad-band emission that spans the full bandwidth of the UWL. In Section 2, we describe the Murriyang observations and data reduction. Our results are then presented in Section 3. We discuss the implications of our results in Section 4, followed by a summary in Section 5.

2 OBSERVATIONS AND DATA REDUCTION

We followed up 2XMM J104608.7−594306 with the Murriyang/Parkes UWL for a total of 36 h between 2025 April and 2025 November. The date and duration of each observation are shown in Fig. A1. As can be seen, most observations lasted 1–2 h on a single day, and the longest observation took place on 2025 October 8 with a duration of 6 h. The Murriyang observations were recorded in the pulsar search mode with a sampling time of 256 μs and a frequency resolution of 1 MHz (i.e. 3328 channels across the full bandwidth). The data were coherently dedispersed to the dispersion measure (DM) of 98.41 pc cm^{-3} and stored in 8-bit PSRFITS files (A. W. Hotan, W. van Straten & R. N. Manchester 2004) with full Stokes information. A 2-min scan of a linearly polarized noise diode was performed prior to each observation.

We split the full band of the Murriyang observations evenly into eight sub-bands, each with a bandwidth of 416 MHz. We searched the sub-banded data for single pulses with ±10 pc cm^{-3} around the nominal DM of 98.41 pc cm^{-3} using TRANSIENTX[1] (Y. Men & E. Barr 2024). The DM step size was set to 0.1 pc cm^{-3}, and the maximum boxcar width to 100 ms. We visually inspected all candidates with a peak S/N > 8 (as defined in D. R. Lorimer & M. Kramer 2004) and identified a single bright pulse on 2025 April 7, as indicated in Fig. A1. In order to perform a cross-check, we repeated the single pulse search using PRESTO (S. M. Ransom 2001). We redetected the bright pulse on 2025 April 7, and no other pulses were found. We checked the notices of all-sky high-energy monitors including *Swift*-BAT (H. A. Krimm et al. 2013), *Fermi*-GBM (C. Meegan et al. 2009), and INTEGRAL (P. L. Jensen et al. 2003), and did not find high-energy flares at the time of the Murriyang burst.

We searched each of the Murriyang observations with the Fast Folding Algorithm (FFA; V. Morello et al. 2020) as 2XMM J104608.7−594306 may emit weak regular periodic signals. The data were cleaned and dedispersed to the nominal DM using TRANSIENTX, and then searched using the RFFA utility of the RIPTIDE[2] package over a period range of 0.1–100 s and a duty-cycle range of 0.2 per cent–20 per cent. We folded all candidates with S/N > 8 for manual inspection, and found no periodic signals of astrophysical origin in any of the Murriyang observations. We also conducted a periodicity search using the ACCELSEARCH routine from PRESTO[3] (S. M. Ransom 2001), summing up to 32 harmonics. The resulting candidates were folded and visually inspected, and no astrophysical signals were found. However, using the longest Murriyang observation allowed us to place deep constraints on any periodic emission from 2XMM J104608.7−594306. Given that the system equivalent flux density of the UWL receiver on Murriyang was measured to be 33–72 Jy depending on the frequency (G. Hobbs et al. 2020), the 6 h observation on 2025 October 8 corresponds to a sensitivity limit of ∼50μJy for an 8σ detection threshold based on the radiometer equation, considering a duty cycle of 10 per cent and an effective bandwidth of 773 MHz (excluding flagged channels) within the lower UWL band (0.7–1.7 GHz).

3 RESULTS

We discovered a bright radio burst in the 36 h follow-up observations of 2XMM J104608.7−594306 with Murriyang, as shown in Fig. 1. Considering the complex morphology and sub-components in the burst, we used DM_PHASE[4] (A. Seymour, D. Michilli & Z. Pleunis 2019), a DM optimization algorithm that maximizes the coherent power across the bandwidth, to measure the DM. We dedispersed the burst over a trial DM range of 95–105 pc cm^{-3}with a step size of 0.1 pc cm^{-3}, and obtained a structure-maximizing DM of 99.40 ± 0.07 pc cm^{-3}. This value is consistent with the DM measurement for the MeerKAT burst within 1σ (K. M. Rajwade et al. 2025).

3.1 Burst morphology

The Murriyang burst from 2XMM J104608.7−594306 shows a similar unusual emission profile to the MeerKAT burst (K. M. Rajwade et al. 2025): an extremely sharp rise and a slowly decaying morphology, as shown in Fig. 1. Yet, the Murriyang burst comprises more sub-components, including a precursor prior to the brightest component, which is not observed in the MeerKAT burst (see Fig. B1 for a comparison). This precursor is about nine times fainter than the brightest component. Such a feature would be invisible in the MeerKAT data due to the lower S/N.

[1] https://github.com/ypmen/TransientX

[2] https://github.com/v- morello/riptide
[3] https://github.com/scottransom/presto
[4] https://github.com/danielemichilli/DM_phase

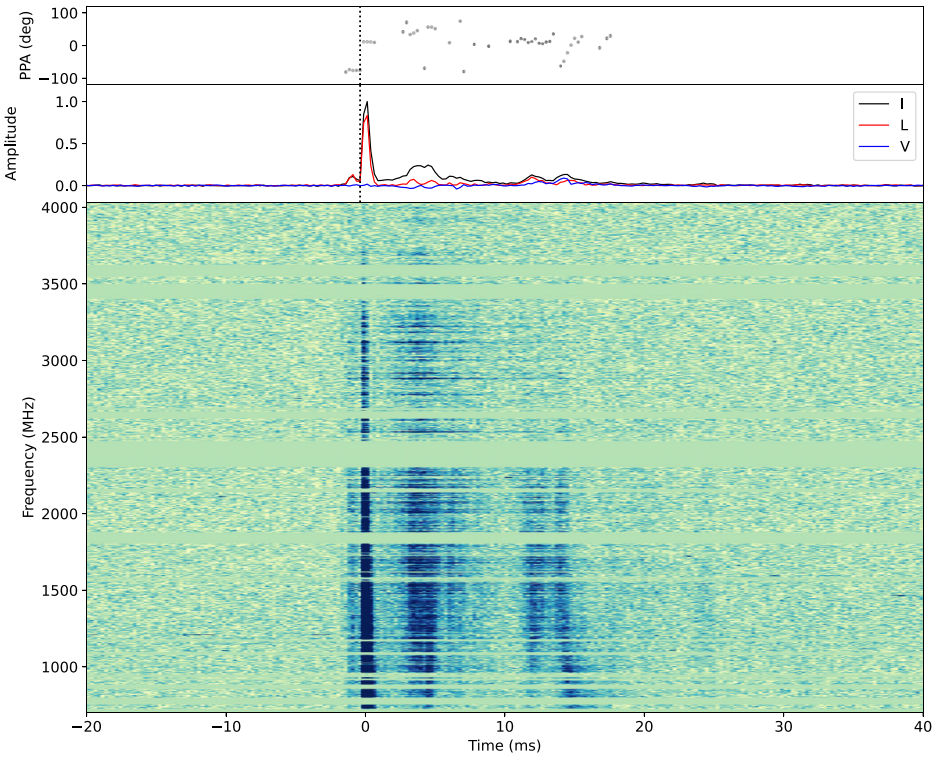

Figure 1. Murriyang/Parkes detected radio burst from 2XMM J104608.7−594306. The bottom panel shows the dynamic spectrum, the middle panel shows the frequency averaged pulse profile for total intensity (I), linear polarization (L) and circular polarization (V), and the top panel shows the polarization position angle. The pulse has been coherently dedispersed to the structure maximizing DM of 99.40 pc cm^{-3}, and the polarization data have been Faraday corrected to the rotation measure of −49.3 rad m^{-2}. The dotted vertical line in the top and middle panel indicates the time of the orthogonal jump. Blank horizontal lines in the bottom panel indicate data which were flagged due to the presence of RFI.

Both bursts from 2XMM J104608.7−594306 show temporal structures similar to the quasi-periodic microstructure seen in radio-emitting NSs (I. Pastor-Marazuela et al. 2023b; M. Kramer et al. 2024), which may reflect disturbances in the magnetosphere induced by activity in the NS crust (Z. Wadiasingh & C. Chirenti 2020) or intrinsic angular patterns in the beamed radio emission (M. Kramer, S. Johnston & W. van Straten 2002).

To investigate the microstructure observed in the Murriyang burst, we generated the power spectrum of the burst pulse profile using `Stingray` (M. Bachetti et al. 2024). We modeled the spectrum with both a single and a broken power law, each including a white noise component. The broken power law model is preferred to fit the power spectrum, resulting in lower Bayesian (BIC) and Akaike (AIC) information criteria. In contrast, the single power law model requires a negative white noise constant, which is non-physical and indicates that the curvature of the power spectrum cannot be adequately captured with a simple power law. The break frequency in the broken power law model is located at 0.9 ± 0.1 kHz, corresponding to a characteristic time-scale of 1.1 ± 0.1 ms. This suggests the pulse profile has a typical microstructure time-scale rather than a strict periodicity.

We also performed a periodicity search by fitting the times of arrival (ToAs) of the burst components as a function of component number with a linear function, allowing for gaps between components, following the method described in I. Pastor-Marazuela et al. (2023b). Because of the complexity of the burst morphology, the ToAs were taken to be the peak times of the pulse profile components, with the time resolution adopted as the uncertainty, rather than fitting a multicomponent Gaussian model. This procedure identified 12 components with gaps, corresponding to the component index vector $n = (0, 1, 2, 3, 4, 5, 7, 8, 10, 11, 13, 17)$ and a mean separation of 1.91 ms. To assess the significance of the periodicity, we simulated 10 000 sets of random component ToAs with waiting times drawn from a Poissonian distribution with the same mean spacing and an exclusion parameter $\eta = 0.2$. We fitted those simulated ToAs to the same linear function as the data, and compared the reduced χ^2 statistic. The resulting significance is 2.2σ, well below the 3σ threshold typically required to claim a periodic signal.

Since the characteristic time-scale inferred from the power spectrum analysis differs from the inferred mean component separation obtained from the ToA fitting, and the latter periodicity test results in a significance below the 3σ threshold, the burst structure does not show evidence for a strictly periodic structure.

We do not see evidence of scattering in the brightest and narrowest component of the Murriyang burst (see Fig. 1), consistent with that observed in the MeerKAT burst. Any underlying scattering in the radio emission should have a time-scale shorter than the width of the narrowest component (0.5 ms).

3.2 Spectrum

To measure the flux density of the burst, we calibrated the Murriyang data using the flux calibrator PKS B1934−638, following the method described in S. Dai et al. (2019). We measured the peak flux density to be 30.03 ± 0.12 Jy, where the uncertainty was estimated using the standard deviation of the baseline noise. This

is ∼100× brighter than the MeerKAT burst, and corresponds to a radio luminosity of $\sim 2 \times 10^{32}$ erg s^{-1} assuming isotropic emission and a source distance of 1.5 kpc. We defined the on-pulse region as the interval between the first and last sample with a flux density greater than three times the noise level, and obtained a burst duration of 33.5 ms. Integrating the flux density over the on-pulse region we obtained a fluence of 66.4 ± 4.0 Jy ms.

We analysed the spectrum of the entire burst by dividing the Murriyang data into 13 × 256 MHz sub-bands and measuring the flux density in each sub-band. We assumed that the burst duration does not change across the sub-bands. We also assumed that each sub-band contains many scintles that our analysis is not limited by scintillation. This is likely to be true given that the NE2001 model (J. M. Cordes & T. J. W. Lazio 2002) predicts a scintillation bandwidth of only ∼200 Hz at 1 GHz along the line of sight of 2XMM J104608.7−594306. We fitted the spectrum with a simple power-law function, $S_\nu \propto \nu^\alpha$, and obtained a spectral index of $\alpha = -2.18 \pm 0.16$. We also measured the spectral indices of the different components in the burst and obtained values ranging between -2.63 ± 0.16 and -1.72 ± 0.11. No monotonic evolution of the spectral index was observed.

3.3 Polarimetry

We created a full-Stokes PSRFITS format archive for the burst by extracting the Murriyang data using DSPSR (W. Straten & M. Bailes 2011). Approximately 25 per cent of the 3328 frequency channels were flagged using PSRCHIVE (A. W. Hotan et al. 2004) due to radio frequency interference (RFI). The data were polarization calibrated using the 2-min noise diode observation. We measured the Faraday rotation in the Stokes data using the RMSYNTH tool from the PSRSALSA[5] software suite (P. Weltevrede 2016). We searched a broad range of rotation measures (RMs) between ±10000 rad m^{-2} with a step size of 0.1 rad m^{-2}, and obtained a value of -49.3 ± 0.2 rad m^{-2}. This is consistent with the RM measurement for the MeerKAT burst within 1σ (K. M. Rajwade et al. 2025).

After correcting for the Faraday rotation, we created the polarimetric pulse profile using PSRSALSA, as shown in Fig. 1. Bias in the linear polarization L was removed for each sample following the method in J. F. C. Wardle & P. P. Kronberg (1974), and the polarization position angles (PPAs) were measured for samples with $L > 3\sigma$, where σ is the off-pulse noise. We averaged L/I and $|V|/I$ across the pulse profile and obtained a linear and circular polarization fraction of 0.54 ± 0.02 and 0.22 ± 0.01, respectively. Parts of the burst show nearly 100 per cent polarization (e.g. in the precursor component), suggesting that the emission is produced by coherent curvature radiation (S. M. Rahaman, D. Mitra & G. I. Melikidze 2022). We see variations in the PPA across the pulse profile in Fig. 1. In particular, there is a PPA jump between the precursor and the brightest component, as indicated by the dotted vertical line. We used the mean values of PPAs before and after the jump to calculate the jump angle. This resulted in a value of $87.2^\circ \pm 1.4^\circ$. The uncertainty was computed from the standard deviation of PPAs weighted by the errors in the PPA measurements and based on the principle of error propagation. The observed PPA jump is consistent with an orthogonal jump within the 2σ error range, which has been observed in many pulsars (R. N. Manchester, J. H. Taylor & G. R. Huguenin 1975; J. M. Cordes, J. Rankin & D. C. Backer 1978; D. C. Backer & J. M. Rankin 1980; D. R. Stinebring et al. 1984; A. Karastergiou 2009) and some FRBs (J. C. Jiang et al. 2024; J. R. Niu et al. 2024). This further corroborates the NS nature of 2XMM J104608.7−594306.

[5] https://github.com/weltevrede/psrsalsa

4 DISCUSSION

2XMM J104608.7−594306 exhibits many characteristics similar to those seen in radio-loud magnetars: transient radio emission, complex burst morphology with multiple emission components, high linear polarization, and significant brightness variability between the Murriyang and MeerKAT bursts. The spectral index we measured is steeper than the spectral indices of most magnetars that typically range from −0.5 to +0.3 (K. Lazaridis et al. 2008; P. Torne et al. 2015; S. Dai et al. 2019), but similar to Swift J1818.0−1607 (M. E. Lower et al. 2020). Meanwhile, the radio luminosities of the Murriyang and MeerKAT bursts are comparable to the average radio luminosity of radio-loud magnetars (V. M. Kaspi & A. M. Beloborodov 2017; P. Esposito et al. 2021). These suggest that 2XMM J104608.7−594306 could represent an evolutionary link between XDINSs and magnetars.

Alternatively, considering the X-ray luminosity of 2XMM J104608.7−594306 is consistent with that of CCOs (A. De Luca 2017), 2XMM J104608.7−594306 could be a CCO candidate. However, identifying a supernova remnant in the Carina Nebula is difficult due to interactions of strong winds of massive stars with their environments and the extinction at optical and infrared wavelengths (L. K. Townsley et al. 2011). Given that most CCOs show fast spin periods of 0.1–0.4 s and weak dipolar magnetic fields of $\sim 10^{11}$ G (V. E. Zavlin et al. 2000; E. V. Gotthelf, J. P. Halpern & F. D. Seward 2005; E. V. Gotthelf & J. P. Halpern 2009), finding the spin period and period derivative of 2XMM J104608.7−594306 will allow us to confirm its nature. We did not find persistent pulsed radio emission above ∼50 μJy in the Murriyang observations. This limit is comparable to the flux density of the faint pulsed radio emission recently detected from the CCO 1E 1207.4−5209 (33 μJy at 816 MHz; L. Zhang et al. 2025). Also, 2XMM J104608.7−594306 and 1E 1207.4−5209 are located at similar distances. Given these considerations, we cannot rule out the presence of radio pulsations from 2XMM J104608.7−594306, and more sensitive observations in the time domain are required to probe this further.

We identified an orthogonal jump in the PPA of the Murriyang burst. This is similar to the orthogonal PPA jumps seen in pulsars, which can be explained by the superposition of the O-mode and X-mode waves that are separated by 90° in the highly magnetized magnetosphere (J. J. Barnard & J. Arons 1986). Both coherent and incoherent superpositions of the two orthogonal modes are possible. While the coherent superposition allows for non-orthogonal jumps and the existence of circular polarization (J. Dyks 2017), the incoherent superposition predicts depolarization at the jump time (S. Singh, Y. Gupta & K. De 2024). We do not observe significant depolarization when the PPA jump happens in Fig. 1. This may be attributed to our limited sampling time of 256 μs, which is insufficient to resolve the PPA jump. Consequently, we cannot distinguish between the coherent and incoherent superpositions for the PPA jump observed here. We use the short time-scale of the PPA jump to derive a generic constraint on the emission region. The time-scale of <256 μs corresponds to a light-crossing length of <77 km. This is much smaller than the light cylinder radius of typical pulsars (D. R. Lorimer & M. Kramer 2004), consistent with the radio emission arising from the NS magnetosphere.

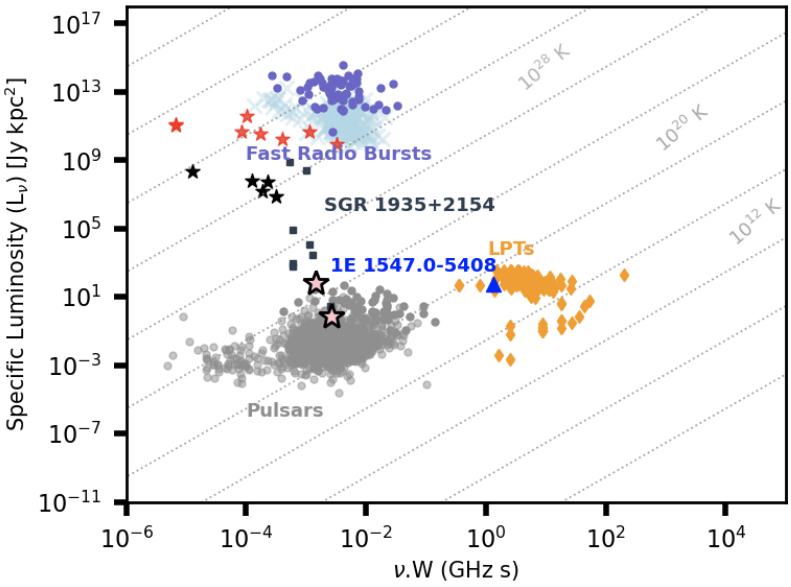

Figure 2. Phase space of various coherent radio transients. The brightest components of the two bursts detected by MeerKAT and Murriyang from 2XMM J104608.7−594306 are shown by the pink stars. The dotted grey lines represent lines of constant brightness temperatures. The data points for FRB 20180916B (red stars), FRB 20121102A (light blue crosses), FRB 20200112E (black stars), one-off FRBs (purple points), SGR 1935+2154 (black squares), 1E 1547.0−5408 (blue triangle), pulsars (grey points) and LPTs (yellow diamonds) are taken from M. Caleb et al. (2024), G. L. Israel et al. (2021), K. Nimmo et al. (2022) and references therein.

The dynamic spectrum of the second radio burst reveals peculiar radio emission that is reminiscent of some features that are exhibited by repeating FRBs. For example, similar to the discovery burst, the dynamic spectrum shows multiple emission components with subsequent emission components becoming visible at lower radio frequencies. In the discovery paper, K. M. Rajwade et al. (2025) discuss this behaviour as a manifestation of localized emission components having different spectral indices. However, since there is no evidence of spectral evolution here (see Section 3.2), the chronological trend in the occurrence of emission at lower frequency favours the possibility that this feature is intrinsic to the emission mechanism. Furthermore, when the second burst is corrected for dispersion using the structure-maximizing DM, the trailing component shows evidence for being underdedispersed. Similar behaviour has been seen in a small sample of radio bursts of multiple repeating FRBs (e.g. M. Caleb et al. 2020; Z. Pleunis et al. 2021; V. R. Marthi et al. 2022). These observables further add credence to the suggestion that these bursts share the same emission mechanism with the FRB-like burst events seen from SGR J1935+2154 (F. Kirsten et al. 2021; U. Giri et al. 2023; W. Zhu et al. 2023).

We compare the isotropic-equivalent spectral luminosity of the brightest component in the two bursts detected by Murriyang and MeerKAT from 2XMM J104608.7−594306 with other short-duration radio transients in Fig. 2. The brightest component in the MeerKAT burst is comparable in luminosity to the brighter pulsars. This is also consistent with the typical radio fluxes observed from radio magnetars. On the other hand, the Murriyang burst is two orders of magnitude brighter than the MeerKAT burst, similar to the luminosity jumps seen in the bright bursts from SGR J1935+2154 (F. Kirsten et al. 2021), the NS that emitted two FRB-like bursts and comparable to the bright radio burst from another magnetar 1E 1547.0−5408 (G. L. Israel et al. 2021). Given the luminosity of the Murriyang burst and the observational similarities to repeating FRBs, we speculate that these bursts may share the same emission mechanism to sporadic bright bursts observed from SGR J1935+2154 (F. Kirsten et al. 2021). If we assume that the magnetic field powers these bursts (Y. Lyubarsky 2020; Y. Yuan et al. 2020), we predict that the same mechanism operates over multiple orders of magnitude in magnetic field strength. Assuming that the radio luminosity is some fraction of the total magnetic energy of the star ($\sim k \int \frac{B^2(r)}{2\mu_0}\, \mathrm{d}^3 r$ where $k \ll 1$), the expected luminosity of the burst can be at least 4–5 orders of magnitude smaller than the brighter bursts seen from SGR J1935+2154 if the magnetic field strength for 2XMM J104608.7−594306 is a factor of 100 smaller. This is consistent with the estimated luminosities for the bursts presented in this work.

We estimate the radio burst rate of 2XMM J104608.7−594306 to be $0.05^{+0.13}_{-0.04}\,\mathrm{h}^{-1}$ above the Murriyang sensitivity limit of ∼0.3 Jy. The uncertainties are computed at 95 per cent confidence level assuming Poisson statistics. This burst rate is higher than those estimated from the monitoring campaign of magnetars with a sensitivity limit of ∼7.5 Jy at 408 MHz ($<226-785\,\mathrm{yr}^{-1}$; A. Geminardi et al. 2025).

5 SUMMARY

In this paper, we report the detection of a bright and wideband radio burst from 2XMM J104608.7−594306 using the Murriyang UWL receiver. The burst is two orders of magnitude brighter than the original burst detected by MeerKAT 14 months prior. The burst shows a fast rising, slowly decaying morphology and emission across the full UWL bandwidth with a spectral index of $\alpha = -2.18 \pm 0.16$. We find microstructure in the burst on a typical time-scale of 1.1 ms with no evidence of periodicity. Polarimetric

analysis shows the burst is 54 per cent linearly polarized and 22 per cent circularly polarized. We identify an orthogonal jump in the PPAs, consistent with the emission arising from the NS's magnetosphere. The peak luminosity is brighter than most pulsars and comparable to some of the bright bursts of SGR 1935+2154. If this emission is magnetically powered, it suggests that the underlying emission mechanism could operate over a wide range of magnetic field strengths and radio luminosities. Our discovery of two bursts from 2XMM J104608.7−594306 – detected by Murriyang and MeerKAT, respectively – demonstrates that radio-quiet NSs such as XDINSs and CCOs may emit rare, sporadic radio emission and highlights the need for regular monitoring of these objects.

ACKNOWLEDGEMENTS

The Parkes radio telescope (Murriyang) is part of the Australia Telescope National Facility that is funded by the Australian Government for operation as a National Facility managed by CSIRO. We acknowledge the Wiradjuri people as the traditional owners of the Observatory site. JT thanks Shi Dai for support and guidance with the flux calibration of the UWL data. KMR acknowledges support from a UKRI-STFC grant (SKA-NIPS, no. ST/Z510439/1). JT and BWS acknowledge funding from an STFC Consolidated grant. MC and KS acknowledge support of an Australian Research Council Discovery Early Career Research Award (project number DE220100819) funded by the Australian Government. IPM further acknowledges funding from an NWO Rubicon Fellowship, project number 019.221EN.019. This research has made use of NASA's Astrophysics Data System Bibliographic Services.

DATA AVAILABILITY

The raw UWL data will be available to download via the CSIRO Data Acess Portal (https://data.csiro.au/) following an 18-month proprietary period. Other data products will be shared on reasonable request to the corresponding author.

REFERENCES

Bachetti M. et al., 2024, J. Open Source Softw., 9, 7389
Backer D. C., Rankin J. M., 1980, ApJS, 42, 143
Barnard J. J., Arons J., 1986, ApJ, 302, 138
Bochenek C. D., Ravi V., Belov K. V., Hallinan G., Kocz J., Kulkarni S. R., McKenna D. L., 2020, Nature, 587, 59
CHIME/FRB Collaboration, 2020, Nature, 587, 54
Caleb M. et al., 2020, MNRAS, 496, 4565
Caleb M. et al., 2024, Nat. Astron., 8, 1159
Cordes J. M., Lazio T. J. W., 2002, preprint (arXiv:astro-ph/0207156)
Cordes J. M., Rankin J., Backer D. C., 1978, ApJ, 223, 961
Dai S. et al., 2019, ApJ, 874, L14
De Luca A., 2017, J. Phys. Conf. Ser., 932, 012006
Dyks J., 2017, MNRAS, 472, 4598
Esposito P., Rea N., Israel G. L., 2021, in Belloni T. M., Méndez M., Zhang C., eds, Astrophysics and Space Science Library, Vol. 461, Timing Neutron Stars: Pulsations, Oscillations and Explosions. Springer-Verlag, Berlin, p. 97
Geminardi A. et al., 2025, A&A, 700, A19
Giri U. et al., 2023, preprint (arXiv:2310.16932)
Gotthelf E. V., Halpern J. P., 2009, ApJ, 695, L35
Gotthelf E. V., Halpern J. P., Seward F. D., 2005, ApJ, 627, 390
Haberl F., 2007, Ap&SS, 308, 181
Hobbs G. et al., 2020, Publ. Astron. Soc. Aust., 37, e012
Hotan A. W., van Straten W., Manchester R. N., 2004, PASA, 21, 302
Israel G. L. et al., 2021, ApJ, 907, 7
Jensen P. L., Clausen K., Cassi C., Ravera F., Janin G., Winkler C., Much R., 2003, A&A, 411, L7
Jiang J. C. et al., 2024, National Science Review, 12, nwae293
Karastergiou A., 2009, MNRAS, 392, L60
Kaspi V. M., 2010, Proc. Natl. Acad. Sci., 107, 7147
Kaspi V. M., Beloborodov A. M., 2017, ARA&A, 55, 261
Kirsten F. et al., 2021, Astron. Telegram, 14605, 1
Kondratiev V. I., McLaughlin M. A., Lorimer D. R., Burgay M., Possenti A., Turolla R., Popov S. B., Zane S., 2009, ApJ, 702, 692
Kramer M., Johnston S., van Straten W., 2002, MNRAS, 334, 523
Kramer M., Liu K., Desvignes G., Karuppusamy R., Stappers B. W., 2024, Nat. Astron., 8, 230
Krimm H. A. et al., 2013, ApJS, 209, 14
Kurpas J. et al., 2025, A&A, 694, A160
Lazaridis K., Jessner A., Kramer M., Stappers B. W., Lyne A. G., Jordan C. A., Serylak M., Zensus J. A., 2008, MNRAS, 390, 839
Lorimer D. R., Kramer M., 2004, Handbook of Pulsar Astronomy, Vol. 4. Cambridge Univ. Press, Cambridge
Lower M. E., Shannon R. M., Johnston S., Bailes M., 2020, ApJ, 896, L37
Lu W.-J., Zhou P., Wang P., Shao Y.-X., Li X.-d., Vink J., Li D., Chen Y., 2024, ApJ, 963, 151
Lyubarsky Y., 2020, ApJ, 897, 1
Manchester R. N., Taylor J. H., Huguenin G. R., 1975, ApJ, 196, 83
Marthi V. R. et al., 2022, MNRAS, 509, 2209
Meegan C. et al., 2009, ApJ, 702, 791
Men Y., Barr E., 2024, A&A, 683, A183
Morello V., Barr E. D., Stappers B. W., Keane E. F., Lyne A. G., 2020, MNRAS, 497, 4654
Nimmo K. et al., 2022, Nat. Astron., 6, 393
Niu J. R. et al., 2024, ApJ, 972, L20
Pastor-Marazuela I., Straal S. M., van Leeuwen J., Kondratiev V. I., 2023a, A&A, 672, A151
Pastor-Marazuela I. et al., 2023b, A&A, 678, A149
Pires A. M., Motch C., Turolla R., Treves A., Popov S. B., 2009, A&A, 498, 233
Pires A. M., Motch C., Turolla R., Schwope A., Pilia M., Treves A., Popov S. B., Janot-Pacheco E., 2012, A&A, 544, A17
Pires A. M., Motch C., Turolla R., Popov S. B., Schwope A. D., Treves A., 2015, A&A, 583, A117
Pleunis Z. et al., 2021, ApJ, 911, L3
Rahaman S. M., Mitra D., Melikidze G. I., 2022, MNRAS, 512, 3589
Rajwade K. M. et al., 2025, ApJ, 985, L3
Ransom S. M., 2001, PhD thesis, Harvard Univ.
Rigoselli M., Mereghetti S., Suleimanov V., Potekhin A. Y., Turolla R., Taverna R., Pintore F., 2019, A&A, 627, A69
Seymour A., Michilli D., Pleunis Z., 2019, Astrophysics Source Code Library, record ascl:1910.004
Singh S., Gupta Y., De K., 2024, MNRAS, 527, 2612
Stinebring D. R., Cordes J. M., Rankin J. M., Weisberg J. M., Boriakoff V., 1984, ApJS, 55, 247
van Straten W., Bailes M., 2011, Publ. Astron. Soc. Aust., 28, 1
Torne P. et al., 2015, MNRAS, 451, L50
Townsley L. K., Broos P. S., Chu Y.-H., Gruendl R. A., Oey M. S., Pittard J. M., 2011, ApJS, 194, 16
Wadiasingh Z., Chirenti C., 2020, ApJ, 903, L38
Wardle J. F. C., Kronberg P. P., 1974, ApJ, 194, 249
Weltevrede P., 2016, A&A, 590, A109
Yoneyama T., Hayashida K., Nakajima H., Matsumoto H., 2019, PASJ, 71, 17
Yuan Y., Beloborodov A. M., Chen A. Y., Levin Y., 2020, ApJ, 900, L21
Zane S. et al., 2011, MNRAS, 410, 2428
Zavlin V. E., Pavlov G. G., Sanwal D., Trümper J., 2000, ApJ, 540, L25
Zhang L. et al., 2025, preprint (arXiv:2512.17214)
Zhu W. et al., 2023, Sci. Adv., 9, eadf6198

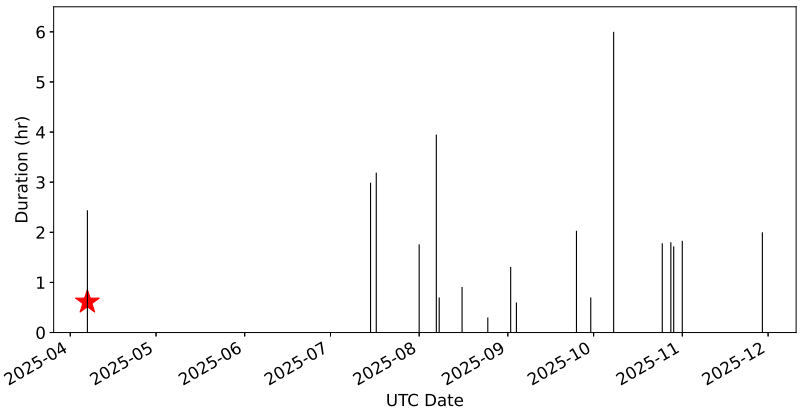

Figure A1. A timeline of targeted Murriyang observations of 2XMM J104608.7−594306. Each vertical line shows the time of an observation, and the height of the line shows the observation duration. The burst detection is marked by a red star.

APPENDIX A: TIMELINE OF THE MURRIYANG OBSERVATIONS

Fig. A1 shows the timeline of the Murriyang observations of 2XMM J104608.7−594306, spanning from 2025 April to 2025 November. The detection of the bright radio burst reported in this paper is marked by a red star.

APPENDIX B: COMPARISON OF THE MURRIYANG AND MEERKAT BURSTS

In Fig. B1, we show the pulse profiles of the two bursts detected by Murriyang and MeerKAT, respectively, with their peaks aligned in time. As the Murriyang observation has a much wider bandwidth (704–4032 MHz) than MeerKAT (856–1712 MHz), we chose to show the pulse averaged over the same frequency range between 856–1712 MHz. We also downsampled the MeerKAT data to the same time resolution as Murriyang, i.e. 256 µs. As the Murriyang burst is much more luminous than the MeerKAT burst, we normalized both bursts by their respective peaks. The second panel shows the difference between the two normalized pulse profiles.

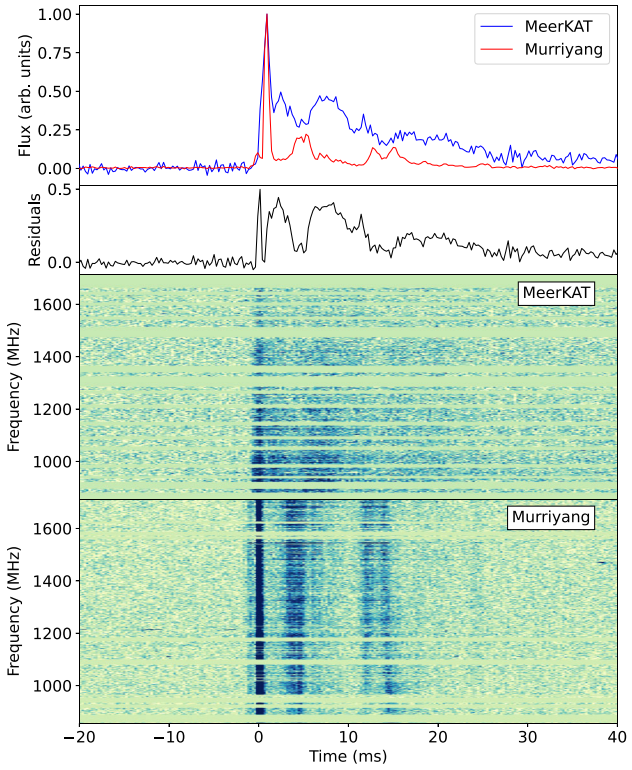

Figure B1. Burst comparison from 2XMM J104608.7−594306 between the MeerKAT and Murriyang bursts over the same bandwidth and at the same spectro-temporal resolution. The top panel shows the pulse profiles averaged over 856–1712 MHz, normalized to the same main peak amplitude (arbitrary units). The second panel displays the residuals after subtracting the pulses. The third panel shows the MeerKAT burst resampled to the Murriyang spectro-temporal resolution, and the bottom panel shows the Murriyang burst at the MeerKAT bandwidth.

This paper has been typeset from a TEX/LATEX file prepared by the author.